



LAWRENCE
LIVERMORE
NATIONAL
LABORATORY

Analysis of Radially Resolved Spectra and Potential for Lasing in Mo Wire Array Z Pinches

S. B. Hansen, A. S. Safronova, J. P. Apruzese, P. D.
LePell, C. Coverdale, C. Deeney, K. B. Fournier, U. I.
Safronova

May 17, 2005

Physics of Plasmas

Disclaimer

This document was prepared as an account of work sponsored by an agency of the United States Government. Neither the United States Government nor the University of California nor any of their employees, makes any warranty, express or implied, or assumes any legal liability or responsibility for the accuracy, completeness, or usefulness of any information, apparatus, product, or process disclosed, or represents that its use would not infringe privately owned rights. Reference herein to any specific commercial product, process, or service by trade name, trademark, manufacturer, or otherwise, does not necessarily constitute or imply its endorsement, recommendation, or favoring by the United States Government or the University of California. The views and opinions of authors expressed herein do not necessarily state or reflect those of the United States Government or the University of California, and shall not be used for advertising or product endorsement purposes.

Modeling of radially resolved spectra and potential for lasing in Mo wire array Z pinches

S. B. Hansen,^{1,2} A. S. Safronova², J. P. Apruzese,³ P. D. LePell,⁴ C. Coverdale,⁵ C. Deeney,⁵
K. B. Fournier,¹ and U. I. Safronova^{2,6}

¹*Lawrence Livermore National Laboratory, Livermore, CA 94551*

²*Physics Department/220, University of Nevada Reno, Reno, Nevada 89557*

³*Radiation Hydrodynamics Branch, Plasma Physics Division, Naval Research Laboratory, Washington, DC 20375*

⁴*KTECH Corporation, Albuquerque, New Mexico 87123*

⁵*Sandia National Laboratories, Albuquerque, New Mexico 87185*

⁶*University of Notre Dame, Notre Dame, Indiana 46566*

Abstract

Measurements of radially resolved L-shell Mo spectra from wire array pinches on Sandia's Z generator are presented and analyzed using a collisional-radiative model. The spectra indicate large radial gradients in density over the ~ 8 -mm-diameter plasma column, but only the emission from the ~ 2 mm central region of the pinch appears to be influenced by opacity. Population inversions and significant gain factors for 100-200 Å transitions in Ne-like Mo are predicted to exist at the diagnosed plasma conditions.

In a recent paper [1], an analysis of axially and temporally resolved L-shell spectra from a series of Mo wire array shots on Z was presented using a collisional-radiative model of O-through Mg-like Mo. The electron temperatures and densities diagnosed from the L-shell Mo spectra indicated significant axial density gradients (with decreasing density toward the cathode end of the ~ 2 cm plasma column) and peak densities occurring just before the peak x-ray emission. In the present work, we complete the analysis of the spectroscopic measurements from the series of 45-, 50-, and 55-mm-diameter nested Mo wire arrays described in Ref. 1 by diagnosing radially resolved spectra from the 50-mm-diameter wire array, which was typical of the series.

Power measurements in the previous work, as well as fundamental atomic physics considerations [2], confirm that L-shell emitters as pulsed power loads have smaller x-ray yields than K-shell emitters with similar photon energies [3,4]. A separate potential point of interest is whether L-shell Z pinch plasmas can achieve conditions relevant to x-ray laser studies: in 1987, Mo plasmas ionized to the L-shell by laser irradiation were established as high-gain ($\sim 4 \text{ cm}^{-1}$) media for collisionally-pumped x-ray lasers [5]. Previous Ne-like x-ray laser schemes on Z-pinches involved the use of Kr gas puffs that were plagued by non-uniformities and absorption due to large plumes of cold Kr gas (see Ref. 6 and references therein). Wire arrays, especially if nested [7,8], could produce a more uniform pinch. Capillary discharges have accomplished this at lower currents, leading to successful demonstrations of lasing for the 469 Å line of Ne-like Ar [9,10]. If the nested Mo wire array plasmas considered here are sufficiently uniform, they may be attractive lasing media for 100-200 Å transitions in Ne-like Mo ions.

Radially resolved L-shell spectra from a nested Mo wire array with a 50 mm outer diameter and a 20 mm length were measured using a pentaerythritol (PET) crystal bent into a 50.8 mm radius. Unwanted light and low energy x-rays were filtered out of the incident beam by 50.8 μm of beryllium (10% transmission at 1.35 keV). A 0.10 mm wide imaging slit oriented parallel to the pinch axis and placed 2/3 of the distance to the instrument from the plasma

source provided radial resolution of 0.3 mm. Because of the crystal's 2-D spacing (8.742 Å), its spectral range was somewhat limited compared to that of the axially and temporally resolved spectra given in Ref. 1: low energy continuum emission was captured down to 2.0 keV but the line emission was cut off at 2.95 keV, as shown in the film image of Fig. 1. The low energy continuum has a 10% intensity diameter of 2.8 mm and a full-width at half-maximum (FWHM) of 1.5 mm. Lineouts dividing the spectrum into four 1-mm regions from the center of the pinch outwards were taken as indicated on Fig. 1.

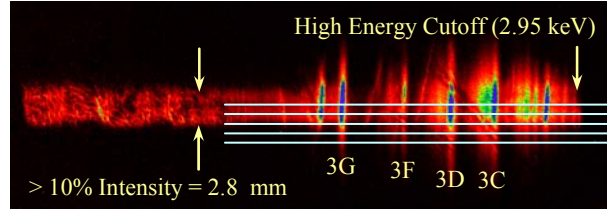


FIG 1. Radially resolved film data from the 50 mm-diameter Mo wire array. The radial extent of intense radiation is indicated by arrows and major lines from the Ne-like charge state are labeled.

Experimental spectra from three of the four diagnosed radial segments are shown as gray lines on the left side of Fig. 2 along with modeled spectra (black lines) at the diagnosed plasma conditions. (The 2-3 mm spectrum, not shown due to space considerations, resembles that of the 3-4 mm spectrum and has a similar quality of fit.) The electron density is diagnosed using a ratio of Ne-like lines $[(3A+3B)/(3F+3G)]$ which increases monotonically with n_e . The temperature is then determined by fitting the relative intensities of the F- and Na-like features indicated in Fig. 2. An advantage of this diagnostic procedure is that it leaves the system underdetermined: by using two ratios to determine two plasma parameters, there remain many features in the modeled emission spectrum that are not explicitly optimized to fit the experimental data and can be used as a cross check of the overall fit. Each spectrum given in Fig. 2 includes a quantitative measure of the overall deviation of the modeled spectra from the data over the 4.0 to 5.5 Å spectral range: $\varepsilon = \Sigma(I_{exp} - I_{mod})^2/N$, where I_{exp} and I_{mod} are the experimental and modeled intensities, respectively (normalized to the F-like feature at 4.5 Å) and N is the number of data points. An average deviation ε less than about 1% indicates a good overall fit.

On the right side of Fig. 2, the diagnosed electron densities (n_e) and temperatures (T_e) for each radial region are given, showing a significant decrease in n_e outward from $4 \times 10^{21} \text{ cm}^{-3}$ at the center of the pinch to $6 \times 10^{20} \text{ cm}^{-3}$ at the edge and a relatively steady T_e between 1.4 and 1.6 keV over the radiating region. The approximate energy emitted in > 1 keV x-rays from each of the radial segments (scaled to sum to half the measured L-shell yield) drops by a factor of ten from the central region of the pinch to the 3-4 mm radius.

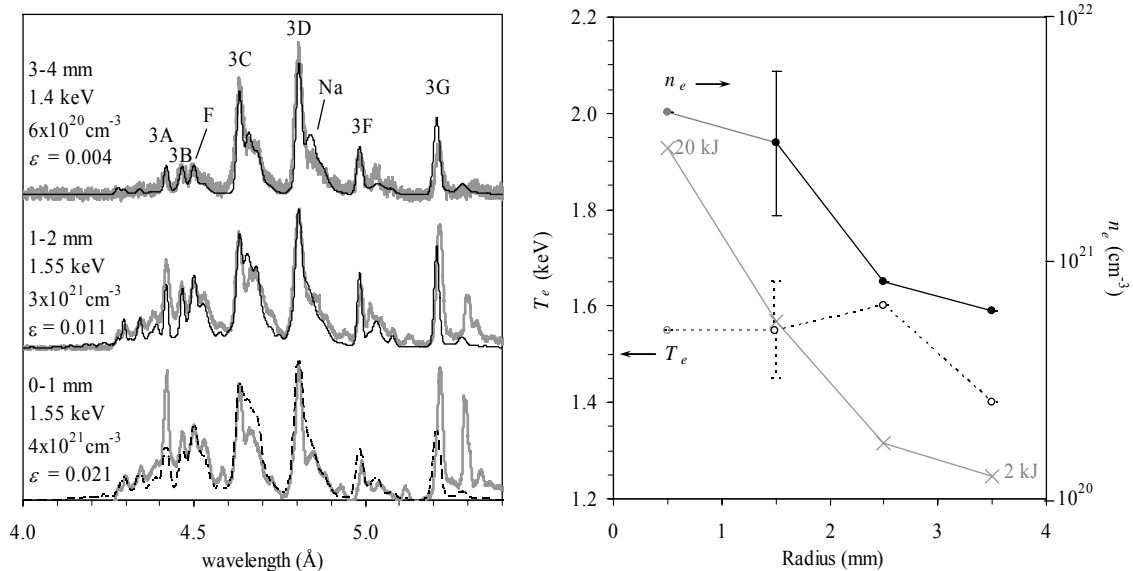


FIG 2. Left panel: selected radially resolved spectra (gray lines) compared with best-fit modeled spectra (black lines). Right panel: diagnosed T_e (open circles, dashed lines) and n_e (closed circles, solid lines) as a function of radius in the Mo wire array, along with estimated total energy emitted in L-shell lines (crosses). Typical error bars are given for the 1-2 mm spectrum. Since the centermost spectrum (0-1 mm) is not well-described by the model, the diagnosed T_e and n_e at that point are unreliable.

The good overall fits for the 1-2 and 3-4 mm spectra (and the 2-3 mm spectra, not shown) offer substantial reassurance that the level structure and coupling processes used in the model are sufficiently complete and that the diagnosed plasma conditions are reliable. In contrast, disagreement in un-optimized features serves as a warning that further plasma effects or atomic processes should be considered. In particular, the disagreement between the 0-1 mm experimental data and the model probably points to the importance of opacity effects in the dense central portion of the pinch [3], where optical depths for the strong 3C and 3D Ne-like lines can reach 100 over a ~ 3 mm pinch diameter. The most accurate modeling of a plasma with such optical depths would include radiative transfer effects, however, the optically thin modeling presented here gives useful first estimates of plasma conditions, indicating a plasma with sufficient density and extent to support significant gain in lasing transitions if population inversions exist.

We have calculated gain factors for six soft x-ray (100 – 200 Å) lasing transitions between levels in the $2s^2 2p^5 3p$ configuration and the $2s^2 2p^5 3s$ configuration of Ne-like Mo (identified in Fig. 3). The population inversions necessary for lasing occur because the upper levels of these transitions cannot decay rapidly to the Ne-like ground state, while the dipole-allowed decay from their lower levels to ground is rapid, giving rise to the 3F and 3G emission lines. We find that population inversions exist up to electron densities of 10^{23} cm^{-3} for temperatures between 1 and 2 keV. The broad range of plasma conditions under which lasing can occur mitigates the uncertainty in the diagnosed plasma parameters.

The gain factors calculated using the present model at the conditions of the laser-produced plasma described in Ref. 5 ($T_e \sim 2$ keV and $n_e \sim 5 \times 10^{20}$ cm^{-3}) agree to within 10% of the 2 - 4

cm⁻¹ values measured in that experiment, offering validation of the model. Since gain increases almost linearly with increasing electron density up to $n_e \sim 10^{22}$ cm⁻³ (as the number density of ions increases along the lasing path) and densities in the Z pinch plasma reach ten times those of the laser plasma, a simple density scaling of the laser plasma experiments would indicate gain factors of 20 - 40 cm⁻¹ for the Z pinch. However, the high kinetic energy of ions in the imploding Z pinch can broaden and detune the lasing transitions through Doppler effects. This effect is minimal in laser plasmas, where $T_{ion} \sim T_e$, but is significant in the Z pinch plasma, where we estimate T_{ion} to be near 125 keV from the observed line widths and 0-D implosion velocities [1]. In the temperature-broadened limit, gain factors are proportional to $1/\sqrt{T_{ion}}$, thus overall we expect gains in the Z pinch plasma to be of the same order as those of the laser plasma in Ref. 5. A final consideration is the large radial density gradient in the Z pinch plasma column, which will tend to refract lasing emission away from the region of maximum gain. We estimate refraction effects following Ref. [10], where, for cylindrical geometry, the effective gain is $g_0 - (2/L_x)\sqrt{(n_e/n_{ec})}$ with g_0 the gain at uniform density, L_x the density gradient scale length (1 mm), and n_{ec} the critical electron density for the lasing transition ($n_{ec} > 10^{24}$ cm⁻³ for $\lambda < 200$ Å). Refraction reduces the calculated gain factors by 20- 40%.

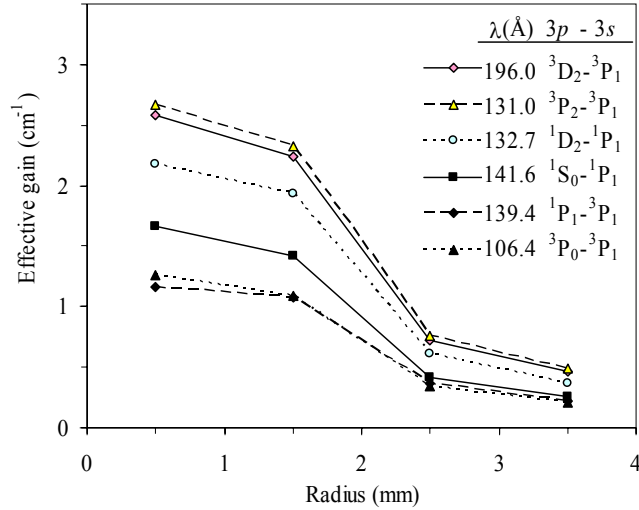


FIG 3. Calculated effective gain factors including 2-D refraction effects as a function of radius for the Mo wire array plasma using the diagnosed conditions given in Fig. 2 and Doppler line shapes with $T_{ion} = 125$ keV.

The effective gain factors from the diagnosed plasma conditions are given in Fig. 3 as a function of radius for the Mo wire array plasma. Effective gains near 3 cm⁻¹ are predicted over the central ~ 4 mm of the plasma column for the 131 and 196 Å transitions and should produce measurable amplification along the axis of the 2 cm wire array plasma. Density gradients at scale lengths below the measured resolution could reduce the predicted gain by refracting the lasing transitions before they are significantly amplified. Photopumping of the lower levels of the lasing transitions in the dense central portion of the pinch may also reduce the gain by as much as a factor of two, according to self-consistent population calculations using escape factors in the slab approximation. On the other hand, if the ion temperature is anisotropic and is much smaller than 125 keV in the axial direction, the gains along axis may be significantly larger than the estimates given here.

Through collisional-radiative diagnostics and modeling of radially resolved spectra from wire array plasmas, we have demonstrated the potential for x-ray lasing in Ne-like Mo on the Z generator. Lasing may also be present in Ni-like [12,13] or Kr-like [14,15] ions in higher-Z wire array plasmas, such as tungsten. It would be worthwhile to field an on-axis spectrometer to look for amplified soft x-ray lines on Z as a ride-along diagnostic. It might even be possible to implement the transient collisional excitation scheme that has been so successful in creating x-ray amplification from laser-produced plasmas [13,16] using the beamlet laser.

Acknowledgements

The authors would like to acknowledge the valuable assistance of D. S. Nielsen, T. C. Moore, and D. O. Jobe for fielding the spectrometers on the Z accelerator, J. E. Bailey and P. W. Lake for their guidance in spectrometer design, operation, and data analysis, and A. Osterheld for helpful discussions. The authors thank J. F. Seamen, R. J. Leeper, R. S. Spielman, M. A. Hedemann, D. H. McDaniel, M. K. Matzen, and J. P. Quintenz for sustained programmatic support. This work was performed under the auspices of the U.S. Department of Energy by University of California Lawrence Livermore National Laboratory under Contract No. W-7405-Eng-48 and by Sandia, a multiprogram laboratory operated by Sandia Corporation, a Lockheed Martin Company, for the United States Department of Energy under Contract No. DE-AC04-94AL85000. The work of S.H. and A.S. was supported in part by Sandia National Laboratories under Contract No. 27625.

References

1. P.D. LePell *et al.*, Phys. Plasmas **12**, 032701 (2005).
2. J. P. Apruzese, Naval Research Laboratory Memorandum Report No. 6720-99-8341, 1999 (unpublished).
3. J. P. Apruzese *et al.*, Phys. Plasmas **5**, 4476 (1998).
4. C. Deeney *et al.*, Phys. Plasmas **6**, 2081 (1999).
5. B. J. MacGowan *et al.*, J. Appl. Phys. **61**, 5243 (1987).
6. J. Davis, R. Clark, J. P. Apruzese, and P. C. Kepple, IEEE Trans. on Plasma Science **16**, 482 (1988).
7. C. Deeney *et al.*, Phys. Rev. Lett. **81**, 4883 (1998).
8. J. Davis, N. A. Gonderenko, and A. L. Velikovich, Appl. Phys. Lett. **70**, 170 (1997).
9. J. J. Rocca *et al.*, Phys. Rev. Lett. **73**, 2192 (1994); J. J. Rocca *et al.*, Phys. Rev. Lett. **75**, 1236 (1995); J. J. Rocca *et al.*, Phys. Plasmas **2**, 2554 (1995).
10. J. J. Rocca, Rev. Sci. Instrum. **70**, 3799 (1999).
11. S.B. Hansen, PhD thesis, University of Nevada, Reno (2003).
12. S. Maxon *et al.*, Phys. Rev. Lett. **63**, 236 (1989); S. Maxon *et al.*, Phys. Rev. Lett. **63**, 1896 (1989).
13. J. Dunn *et al.*, Phys. Rev. Lett. **80**, 2825 (1998).
14. M. Klapisch *et al.*, Physica Scripta **41**, 819 (1990).
15. Yu. V. Afanasiev and V. N. Shlyaptsev, Sov. J. Quantum Electron. **19**, 1606 (1989); V. N. Shlyaptsev *et al.*, Proc.SPIE Int. Soc. Opt. Eng. **2012**, 111 (1993).